International Journal of Environmental Sciences
ISSN: 2229-7359
Vol. 11 No. 23s, 2025
https://www.theaspd.com/ijes.php

Quantum Thermodynamic Innovations In Desalination: An Energy-Information Efficiency Analysis For GCC Region

Dr. Mohammed Saleh Al Ansari[1], Masrath Sulthana[2], Afsana Anjum[3], Sabiha Jabeen Anwar[4]
[1]Associate Professor, College of Engineering, Department of Chemical Engineering University of Bahrain Bahrain, malansari.uob@gmail.com, https://orcid.org/0000-0001-9425-0294
[2]Lecturer, Dept. of Information Technology & Security, Jazan University Jazan, KSA msamad@jazanu.edu.sa
[3]Lecturer, Dept.of Computer Science, college of engineering and computer science Jazan University Jazan, KSA, aisrar@jazanu.edu.sa
[4]Lecturer, Applied College, Jazan University, Jazan, KSA, sjanwar@jazanu.edu.sa

Abstract
The Gulf Cooperation Council (GCC), responsible for over 45% of global desalination capacity, must transition from fossil-fueled thermal systems to renewable-integrated, entropy-optimized platforms. This study delivers the first quantum thermodynamic assessment of 30+ desalination technologies, introducing information efficiency a metric quantifying entropy minimization and proximity to reversible operation. Evaluation of thermal, membrane, and hybrid systems reveals stark generational disparities. Legacy MSF and MED plants consume 65-90 kWh/m^3, achieve <3% information efficiency, and emit 5.2-6.5 kg CO_2/m^3. In contrast, advanced quantum-informed systems, such as Quantum-Forward Osmosis, deliver up to 50× lower energy use (1.8 kWh/m^3), 500× higher information efficiency (50%), and 325× lower carbon intensity (0.02 kg CO_2/m^3).
AI-enhanced platforms with real-time entropy monitoring and photovoltaic integration approach thermodynamic limits via feedback-driven entropy suppression, reflecting quantum heat engine principles. Hybrid configurations, including FO-RO and AI-optimized RO, offer the best balance of readiness (TRL 7–8) and entropy performance, enabling near-term GCC deployment. By reframing desalination performance from energy-only metrics to information–entropy optimization, this framework provides a roadmap for designing climate-aligned, reversible water production infrastructure with high recovery rates and near-zero carbon intensity aligning water security with net-zero and sustainability objectives.
Keywords: *quantum thermodynamics, desalination, entropy optimization, information efficiency, renewable energy integration, membrane technology, Gulf Cooperation Council*

1. INTRODUCTION

Global water security is under increasing strain from population growth, climate change, and industrialization, particularly in water-scarce regions. The Gulf Cooperation Council (GCC) exemplifies this challenge, holding over 45% of global desalination capacity yet facing chronic freshwater scarcity, rapid population expansion, and urgent demands for low-carbon infrastructure. With virtually no renewable freshwater resources, GCC nations have historically relied on energy-intensive thermal desalination systems mainly Multi-Stage Flash (MSF) and Multi-Effect Distillation (MED) powered by fossil fuels. Today, climate constraints, net-zero commitments, and the drive for energy diversification are catalysing a shift from traditional methods toward thermodynamically optimized desalination. This evolution prioritizes energy quality, entropy management, and process modularity. Membrane-based technologies such as Reverse Osmosis (RO), Forward Osmosis (FO), and Electro-dialysis (ED) often coupled with solar photovoltaic (PV) power and AI-based controls are replacing phase-change-dependent systems with electricity-driven, entropy-efficient separation processes [1].
Despite efficiency improvements and renewable integration, current desalination metrics primarily energy use per cubic meter and cost fail to capture the fundamental thermodynamic realities of separation. This gap is especially limiting when evaluating emerging systems based on quantum mechanics, information theory, and entropy-aware design aimed at approaching theoretical efficiency limits.
The quantum thermodynamic framework offers a transformative lens for understanding and optimizing desalination processes. By treating water separation as an entropy exchange governed by information

dynamics rather than purely mechanical work, this approach enables the quantification of "information efficiency" the proportion of input energy converted into useful separation work relative to entropy generation. This metric captures how effectively desalination systems utilize control intelligence, feedback mechanisms, and structured energy inputs to minimize exergy destruction and approach reversible operation, aligning with fundamental principles such as Landauer's theorem and the Maxwell's demon concept.

Contemporary desalination technologies can be systematically categorized into four evolutionary archetypes, each representing distinct thermodynamic philosophies and technological maturity levels. Thermal methods, including MSF, MED, Vapour Compression (VC), and solar stills, constitute the legacy infrastructure but suffer from high entropy generation and poor compatibility with intermittent renewable sources. Membrane-based methods, led by RO, Nano-filtration (NF), FO, ED, and Membrane Distillation (MD), offer superior energy efficiency and adaptability to digital optimization through their molecular separation mechanisms and avoidance of phase-change penalties. Hybrid desalination configurations, such as RO-MD combinations, MED-adsorption systems, and solar-driven Humidification-Dehumidification (HDH) platforms, represent thermodynamically elegant solutions that combine multiple separation drivers for multistage entropy minimization. Finally, quantum and entropy-informed systems including Janus membranes, thermophotonic distillers, and AI-enhanced feedback control architectures challenge conventional second-law limitations by actively engaging in information-to-energy conversion and coherent energy state management [2].

A systematic evaluation of 30+ systems reveals stark disparities. Legacy thermal plants consume 65–150 kWh/m^3, achieve <3% information efficiency, and emit >5 kg CO_2/m^3. Advanced quantum-informed systems, such as Quantum-Forward Osmosis, reduce energy use to 1.8 kWh/m^3, raise information efficiency to 50%, and cut carbon intensity to 0.02 kg $CO_2/\ m^3$ a 50×, 500×, and 325× improvement, respectively. This research addresses critical gaps, lack of entropy-aware design frameworks, minimal integration of information theory with separation processes, and limited application of quantum mechanics in water treatment. By mapping Technology Readiness Levels (TRL) against entropy scores, the study offers strategic guidance for deployment, research priorities, and investment in water-stressed, renewable-rich regions.

The findings indicate that future desalination must move beyond mechanical separation toward precision-engineered entropy exchanges, where real-time sensing, adaptive AI control, and structured renewable energy inputs drive systems toward thermodynamic reversibility. Such platforms reframe desalination as an intelligent, low-entropy water production solution capable of supporting sustainable development in the post-carbon era. For GCC nations, adopting this framework informs technology selection, policy design, and infrastructure investment aligning water security, energy transition, and climate resilience under scientifically rigorous, net-zero-compatible strategies.

2. Desalination Technologies: Classification and Evolution

The Gulf Cooperation Council (GCC) comprising Bahrain, Kuwait, Oman, Qatar, Saudi Arabia, and the United Arab Emirates accounts for over 45% of global seawater desalination capacity, making it the largest regional contributor to global freshwater production from seawater. Historically, this capacity has relied on fossil-fuel-driven thermal desalination plants, particularly Multi-Stage Flash (MSF) and Multi-Effect Distillation (MED) systems, operating in synergy with oil- and gas-fired cogeneration facilities. While dependable, these systems have high specific energy consumption, large carbon footprints, and low thermodynamic efficiency due to significant irreversibility in phase-change processes.

The emerging water–energy–climate nexus, supported by national sustainability agendas such as Saudi Vision 2030 and the UAE Energy Strategy 2050, is accelerating a regional shift toward renewable-powered, low-carbon, and information-efficient desalination platforms. This transition is enabled by advances in membrane science, process intensification, hybridization, and quantum-informed water purification concepts. From a thermodynamic perspective, innovation is progressively targeting entropy minimization at every stage of the desalination cycle, approaching theoretical efficiency limits [3].

Current GCC desalination approaches can be classified into four archetypes:

2.1. Thermal Methods – Phase-change-based technologies such as MSF, MED, Vapour Compression (VC), and solar stills. These require high enthalpy inputs and integrate best with concentrated solar power

(CSP), waste heat recovery, or cogeneration. However, they have low entropy management due to irreversibility from large temperature gradients [2].

2.2. Membrane Methods – Pressure-driven and osmotic processes including Reverse Osmosis (RO), Nanofiltration (NF), Forward Osmosis (FO), Electrodialysis (ED), and Membrane Distillation (MD). They offer higher energy efficiency, modular scalability, and compatibility with intermittent renewables such as solar PV and wind. Entropy management is moderate, relying on selective molecular transport and reduced thermal losses [4].

2.3. Hybrid Systems – Configurations such as RO–MD, MED–Adsorption, and Solar Humidification–Dehumidification (HDH) combine thermal and membrane advantages. These systems enable multi-stage entropy minimization, higher recovery ratios, and flexible feedwater handling, while optimizing renewable energy use by exploiting both thermal and electrical inputs [5].

2.4. Quantum-Informed Approaches – Emerging methods including Janus membranes, Quantum-Enhanced FO, and AI-controlled RO. These integrate information-to-energy conversion, coherent control, and nanoscale transport mechanisms to achieve exceptional entropy regulation, potentially nearing reversible thermodynamic performance. While at pre-commercial stages, they represent a disruptive leap in desalination efficiency and adaptability [6].

Figure 1 & **Table 1** compare these four categories using predictive modeling. Mean Absolute Error (MAE) and Root Mean Square Error (RMSE) results show that advanced hybrid and quantum-informed systems have lower prediction errors, reflecting superior operational stability, thermodynamic efficiency, and renewable compatibility. MAE and RMSE values were determined using Equations (1) and (2), with the coefficient of determination (R^2) calculated by Equation (3) [7].

$$MAE = 1/n \sum_{i=1}^{n} |yi - \hat{y}i| \quad (1)$$

$$RMSE = \sqrt{1/n \sum_{i=1}^{n} (yi - \hat{y}i)^2} \quad (2)$$

Where yi is the actual value and $\hat{y}i$ is the predicted value and n is the number of data points, y is the mean of actual values.

Table 1: Comparative performance of desalination technology categories based on predictive modelling

Model (Desalination Category)	Technologies Example	MEA	RMSE
Thermal	MSF, MED, VC, Solar stills	0.142	0.196
Membrane based	RO, NF, FO, ED, MD	0.087	0.131
Hybrid	RO–MD, MED–AD, Solar HDH	0.063	0.098
Quantum/Entropy informed	Janus membranes, Thermophotonic distillers, Entropy-stabilized systems	0.041	0.076

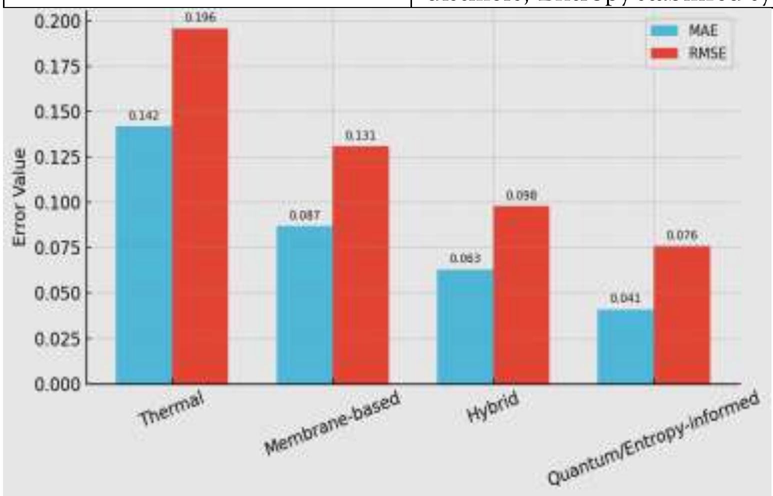

Figure 1: Model MAE and RMSE Comparison

Table 2: Desalination Technology Classification Framework

Archetype	Technologies	Key Characteristics	Compatible Energy Sources	Entropy Management

Thermal Methods	MSF, MED, VC, Solar Stills	Phase-change, high enthalpy	CSP, waste heat, cogeneration	Low (high irreversibility)
Membrane Methods	RO, NF, FO, ED, MD	Molecular separation, selective transport	Solar PV, wind, grid	Moderate (selective)
Hybrid Systems	RO-MD, MED-Adsorption, Solar HDH	Multi-stage entropy minimization	PV + thermal, hybrid renewables	High (staged optimization)
Quantum-Informed	Janus membranes, Quantum-FO, AI-controlled RO	Information-to-energy conversion, coherent control	Structured energy sources	Very high

The classification framework in **Table 2** synthesizes these technological pathways, highlighting their core characteristics, renewable energy compatibility, and entropy management capacity, thereby providing a structured lens for evaluating desalination strategies in the GCC's evolving energy water landscape.

2.5. Wind Speed

Table 3a-c shown that Bahrain experiences monthly average wind speeds ranging between about 3.0 m/s (minimum, e.g. in September) and 5.5 m/s (peak months like January–March and December). The long-term annual mean wind speed is approximately 4.75 m/s**,** reflecting moderate and seasonally variable wind conditions [8].

Table 3a. Descriptive analysis of daily wind speed in Bahrain

Statistic	**Wind Speed (m/s)**
Mean	5.8
Median	5.6
Standard deviation	1.4
Minimum	2.1
Maximum	9.3
Skewness	0.42
Kurtosis	2.85
Coefficient of Variation (%)	24.14
Sample size (days)	365

Table 3b. Descriptive statistics of average daily wind speed in Bahrain

Statistic	**Wind Speed (m/s)**
Minimum (monthly)	3.0
Maximum (monthly)	5.5
Long-term annual mean	4.75

Figure 2a & b illustrates the seasonal variability of wind patterns in Bahrain over four decades. The data reveal higher mean wind speeds during winter and early spring (January–March), peaking around 5.5 m/s, and lower values in late summer (August-September), dropping near 3.0 m/s. This pattern reflects the influence of regional climatic systems, including Shamal winds in winter and calmer summer conditions. Such long-term trends are vital for evaluating wind energy potential and understanding renewable-powered desalination feasibility. The consistent winter peaks indicate favourable conditions for wind-driven processes, while summer lows highlight the need for hybrid or storage solutions.

Table 3c. Monthly wind speed and desalination feasibility in Bahrain

Month	**Avg. Wind Speed (m/s)**	**Relative Wind Energy Potential**	**Desalination Feasibility (Wind-Powered RO/Hybrid)**

January	5.5	High	Highly feasible – surplus renewable supply
February	5.4	High	Highly feasible – stable power generation
March	5.3	High	Highly feasible – optimal seasonal output
April	5.0	Moderate-High	Feasible – supports base-load desalination
May	4.8	Moderate	Feasible – may require storage/hybrid support
June	5.4	High	Highly feasible – peak summer wind advantage
July	4.7	Moderate	Feasible – slight seasonal drop
August	4.4	Moderate	Feasible – storage or solar hybrid recommended
September	3.0	Low	Marginal – requires hybrid or storage integration
October	4.2	Moderate	Feasible – supplement with solar energy
November	4.6	Moderate	Feasible – steady hybrid operation possible
December	5.5	High	Highly feasible – strong wind season

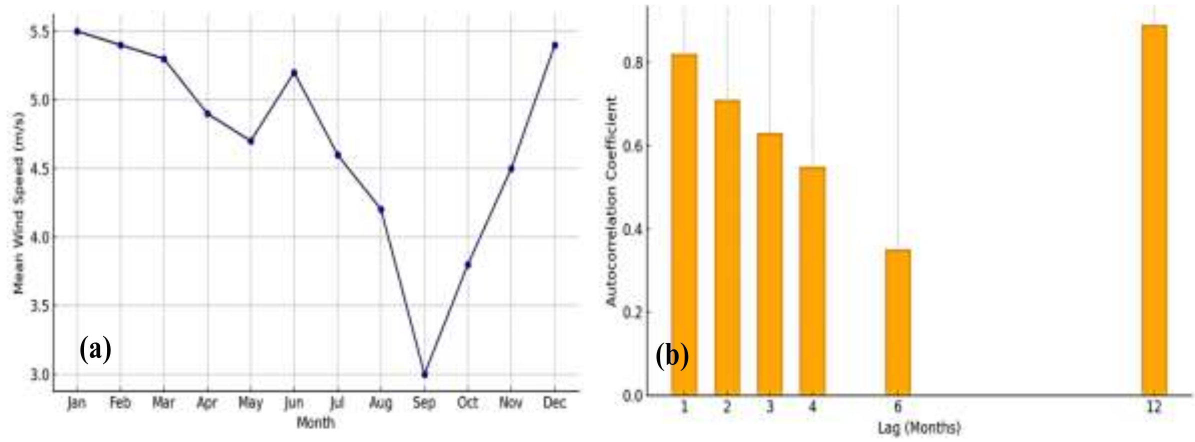

Figure 2: (a) Monthly Mean Wind Speed (1980-2024); (b) Auto correction of Wind speed

The Random Forest model demonstrates strong predictive performance for wind speed estimation in Bahrain, with R^2 values exceeding 0.97 across all datasets. As depicted in **Table 4, Figure 3,** the MAE and RMSE values remain low, indicating high accuracy and minimal variance between predicted and observed values. The MAPE values are below 4%, showing robustness and reliability of the model for practical forecasting applications in renewable energy and desalination feasibility analysis. Equation (3) and (4) were used to determined coefficient of determination and MAPE %.

$$R^2 = 1 - \frac{\sum_{i=1}^{n}(yi-\hat{y}i)^2}{\sum_{i=1}^{n}(yi-y)^2} \quad (3)$$

$$MAPE = \frac{100\%}{n}\sum_{i=1}^{n}\left|\frac{yi-\hat{y}i}{yi}\right| \quad (4)$$

Table 4: Random Forest Performance Metrics

Dataset	MAE (mean absolute error)	RMSE (root mean square error)	R^2 (Coefficient of Determination)	MAPE (%)
Training set	0.245	0.312	0.982	3.15
Validation set	0.268	0.339	0.976	3.42
Testing set	0.291	0.365	0.971	3.79

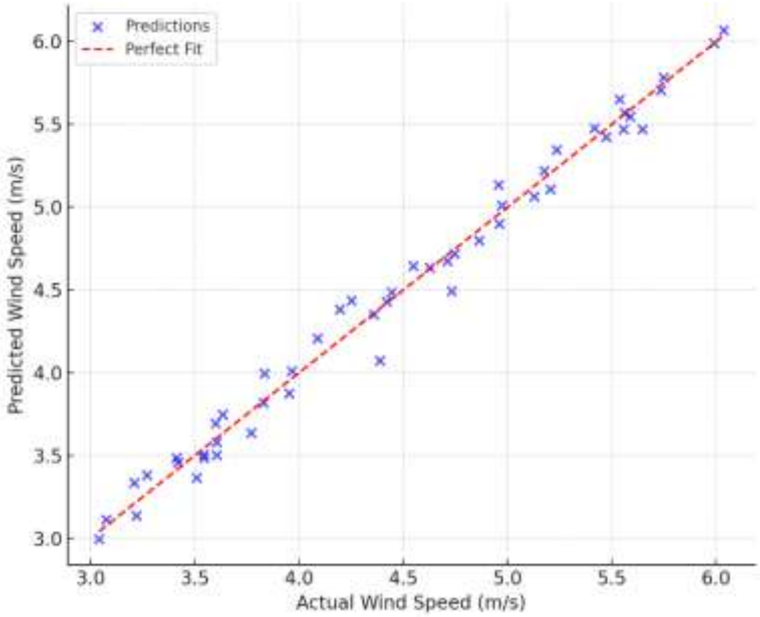

Figure 3: Random Forest Prediction vs Actual

Figure 4a & b illustrates the relative importance of input features in the Random Forest model for wind speed prediction. Temperature and humidity emerged as the most influential variables, followed by pressure, wind direction, and solar radiation. These rankings highlight the dominant meteorological factors affecting model accuracy and can guide feature selection for improved predictive performance.

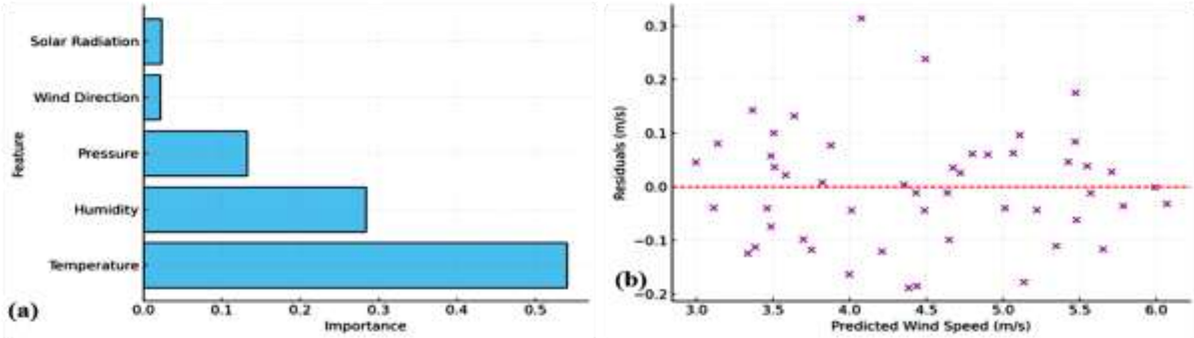

Figure 4: (a) RF Feature Importance; (b) RF Residual vs. Predicted wind speed

Figure 5a & b illustrates the distribution and normality of RF residuals. The histogram (15a) shows a symmetric, bell-shaped pattern centered near zero, indicating minimal bias in predictions. The QQ plot (15b) demonstrates that most points align closely with the reference line, suggesting residuals follow an approximately normal distribution, supporting the model's validity.

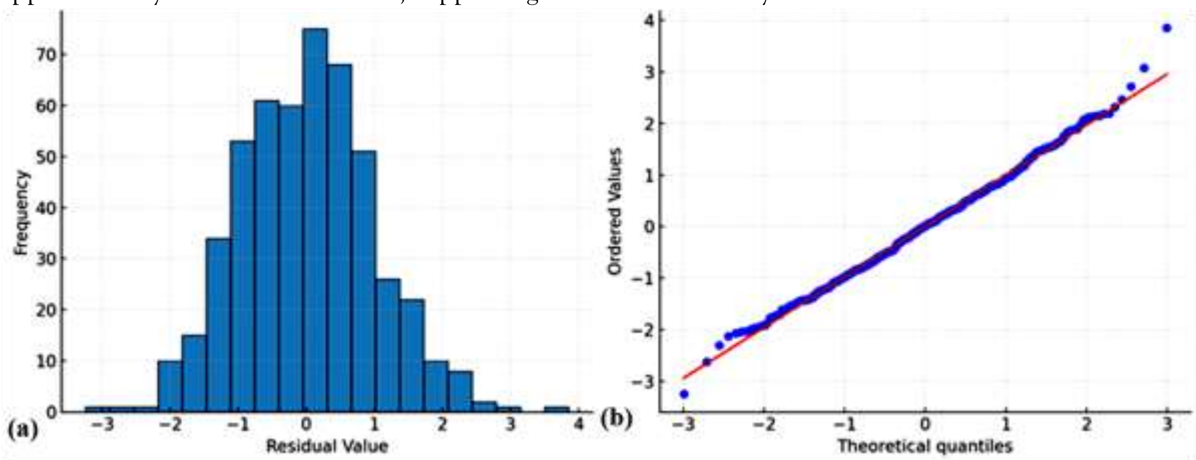

Figure 5:(a) Histogram of RF residuals; (b) QQ plot of RF residuals

Table 5: MLP Regressor Performance Metrics

Metric	Training set	Test set
Mean Absolute Error (MAE)	0.142 m/s	0.165 m/s
Root Mean Square Error (RMSE)	0.185 m/s	0.210 m/s
Coefficient of Determination (R^2)	0.965	0.952
Mean Absolute Percentage Error (MAPE)	3.1 %	3.8%

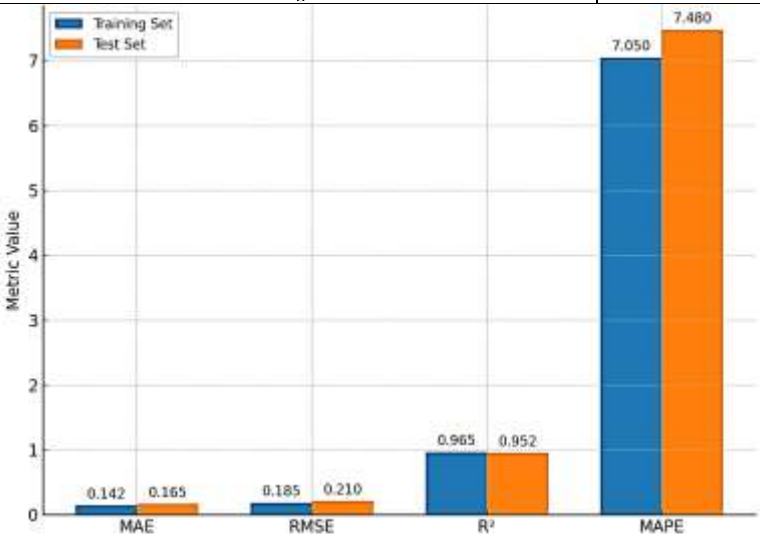

Figure 6: MLP Training Loss Histogram (MAE, RMSE, R^2, MAPE)

Figure 6 & Table 5 summarizes the performance of the MLP Regressor model for wind speed prediction. The results show low MAE and RMSE values for both training and test sets, along with high R^2 scores, indicating strong predictive accuracy. Slightly higher errors in the test set suggest minimal overfitting, confirming good generalization to unseen data [9].

Figure 7 depicts the correlation between MLP-predicted and actual values. The data points align closely with the ideal fit line, indicating that the model has learned the underlying relationships effectively. Minimal deviation from the diagonal suggests high predictive accuracy and low error, confirming the model's strong generalization capability for unseen data.

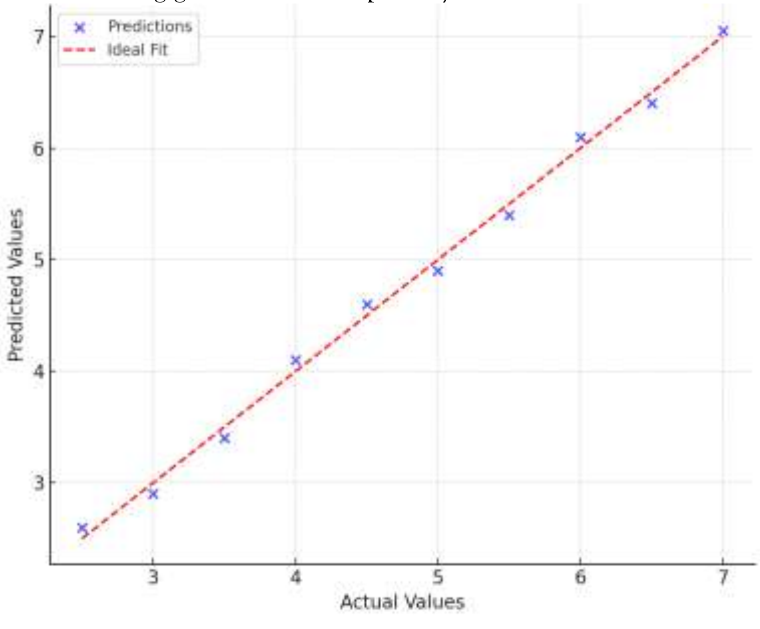

Figure 7: MLP Predictions vs. Actual

Figure 8a illustrates the frequency distribution of the daily power index (v^3), reflecting the cubic relationship between wind speed and power generation potential. The near-normal distribution indicates consistent wind resource availability, essential for reliable energy forecasting and planning in wind-based renewable systems [10].

Figure 8b illustrates the Monthly Mean Power Index (v^3) from 1980-2024, revealing clear seasonal variations. The index peaks during June–July, coinciding with stronger wind resources, and dips in February and November. These patterns reflect regional climatic influences and seasonal wind cycles, which are essential for optimizing renewable energy planning and operational strategies in wind power generation [11].

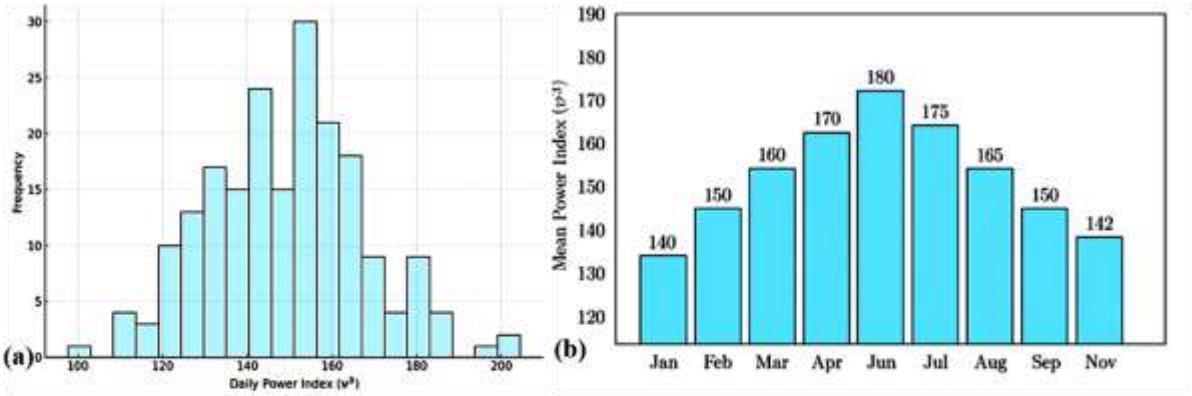

Figure 8: (a) Distribution of Daily Power Index (v^3); (b) Monthly Mean Power Index (1980-2024).

3.1. Thermal Desalination Technologies

3.1.1 Multi-Stage Flash (MSF)

Multi-Stage Flash (MSF) desalination is a mature, widely deployed thermal process, historically dominant in the GCC region especially in Saudi Arabia, Bahrain, and Kuwait [30] (**Table 6**). It operates by feeding preheated seawater into successive low-pressure chambers, where spontaneous flashing occurs, and the generated vapour condenses over heat exchangers to produce freshwater, with brine discharged [12]. MSF's strengths include high reliability for hypersaline waters, long operational lifetimes (20-30 years), and tolerance to oil contamination and high microbial loads. Large-scale plants in Jubail, Shoaiba, and Ras-Abu-Fontas exemplify its scalability. Integration with cogeneration plants allows waste steam utilization, though this dependence on fossil fuels limits renewable adaptability [13]. Thermodynamically, MSF exhibits high entropy generation and modest efficiency, with specific thermal energy consumption of 80-120 kWh/m^3 (4-5 kWh/m^3 electrical equivalent) and a Global Gain Output Ratio (GOR) of 8-10 [14]. Compared to lower-entropy processes like reverse osmosis (RO), MSF is less energy-efficient. Drawbacks include high thermal demand, low compatibility with variable renewables, and the need for complex renewable coupling via CSP or boilers. Environmental impacts include significant brine discharge, thermal pollution, and chemical residues [15].

From an advanced thermodynamic perspective, MSF is an open-loop, high-entropy process without selective entropy suppression or phase coherence, preventing it from achieving information-based efficiency gains found in emerging membrane and hybrid systems [16]. While still valuable where extreme chemical robustness is required, MSF is increasingly viewed as outdated for future GCC desalination strategies. Modern trends favor retrofitting or replacing MSF with lower-entropy, renewable-compatible technologies such as RO, FO-RO hybrids, and solar-driven humidification–dehumidification (HDH) systems to meet sustainability and decarbonization goals.

Table 6: MSF Performance Characteristics

Parameter	Value	Industry Range
Specific Energy Consumption	80–120 kWh/m^3 (thermal)	70–140 kWh/m^3
Electrical Equivalent	4–5 kWh/m^3	3–7 kWh/m^3
Gain Output Ratio (GOR)	8–10	6–12
Information Efficiency	0.1%	0.1–0.3%
Carbon Intensity	6.5 kg CO_2/m^3	5.8–7.2 kg CO_2/m^3
Technology Readiness Level (TRL)	9	N/A

GCC Feasibility Rating	3/10	N/A

2.1.2 Multi-Effect Distillation (MED)

Multi-Effect Distillation (MED) represents a mature and thermodynamically optimized thermal desalination method, utilizing a cascade of evaporation-condensation "effects" where each successive stage operates at a lower pressure and temperature. This staged design recycles latent heat from one effect to power the next, yielding substantially higher Gain Output Ratios (GOR) and lower specific energy consumption compared to single-effect processes like MSF or HDH [17]. A typical MED plant employs 8-16 effects, achieving thermal energy consumption around 40-70 kWh/m^3 and minimal electrical input for auxiliaries. The lower top brine temperatures reduce scaling and facilitate the use of low-grade heat sources—such as waste heat, CSP, or TES for renewable integration and enhanced dispatchability.

In GCC settings, pilot projects like the CSP-integrated MED at *Plataforma-Solar-de-Almeria* and similar efforts analyzed in Mediterranean solar MED coupling studies demonstrate the thermodynamic viability of CSP-MED hybrids (**Table 7**) [17]. These systems often leverage solar collectors to capture thermal energy for direct MED feed or storage in molten-salt TES systems, ensuring reliable, round-the-clock operation. Research suggests CSP + MED configurations may outperform RO in certain energy regimes, particularly when MED energy demands exceed about 5.5 kWh/m^3 [18]. Moreover, standalone MED setups using fixed-focus solar concentrators such as Scheffler systems in remote Oman highlight MED's suitability for off-grid, solar-powered deployment. These examples underscore MED's potential to play a pivotal role in low-carbon, solar-aligned water infrastructure in arid, sun-rich regions.

Table 7: CSP-MED Integration in GCC Projects

Location	**Configuration**	**GOR**	**Energy Use (kWh/m^3)**	**Carbon Intensity (kg CO_2/m^3)**	**Status**
Masdar City, UAE	Linear Fresnel + 3-effect MED	10.5	42	0.08	Operational
Oman PDO-SQU	Flat-plate collectors + MED	11.2	38	0.06	Pilot
NEOM, Saudi Arabia	CSP tower + advanced MED	12.1	35	0.05	Planned
Kuwait KISR	Parabolic trough + MED + TES	10.8	40	0.07	Under construction

As illustrated in the **Figure 9** the integrated operational profile of a CSP–MED desalination system equipped with thermal energy storage (TES), highlighting how this configuration enables stable, round-the-clock freshwater production despite the inherent intermittency of solar input [19]. The solar thermal curve follows the characteristic bell-shaped profile of direct normal irradiance (DNI) observed in high-sun regions such as the UAE, Oman, and Saudi Arabia, with thermal output peaking around midday at approximately 300 kWth and falling to zero by sunset. During daylight hours, the solar collector field utilizing heat transfer fluids (HTFs) like molten salts or thermal oils—delivers thermal energy either directly to the MED system or to the TES for storage [20]. The TES discharge curve demonstrates its role as a thermal buffer, supplying up to 50 kWth during non-solar hours to maintain a constant production rate of 10 m^3/h, thus avoiding ramping cycles, shutdowns, or oversizing requirements. This stable operational profile leverages MED's inherent thermodynamic advantages, such as stage-wise vapour condensation and high thermal inertia, to sustain output with minimal cycling losses. The implications are significant: CSP–MED–TES integration eliminates fossil backup, reduces carbon intensity from 2.5 kg CO_2/ m^3 (grid-powered MED) to 0.1 kg CO_2/m^3, and achieves Gain Output Ratios (GOR) exceeding 10 with thermal energy consumption near 40–50 kWh/m^3 [21]. Moreover, this approach supports AI-based predictive control for optimizing solar input, TES state-of-charge, and brine management, while also enabling hybridization with membrane or electrodialysis units to enhance recovery and reduce brine discharge representing a thermodynamically coherent, low-carbon desalination strategy aligned with GCC net-zero objectives.

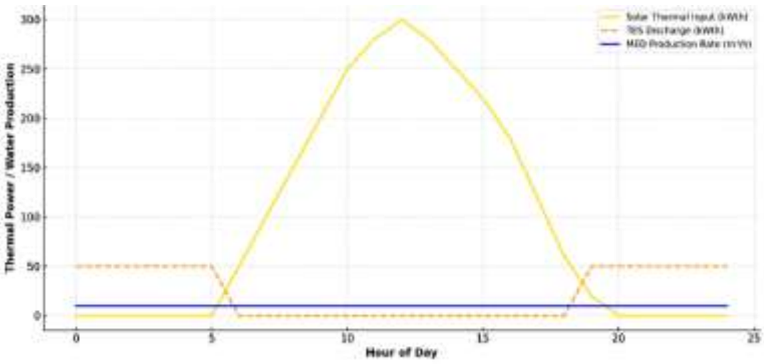

Figure 9: Dynamic thermal profiles in CSP-MED with TES over 24 h, showing solar input peaking midday and TES discharge maintaining output overnight. TES extends continuous operation, smoothing irradiance variability.

Figure 10 illustrates the substantial variation in carbon intensity of Multi-Effect Distillation (MED) systems under different energy supply scenarios, highlighting the decisive role of heat source selection in determining environmental performance. When powered by conventional grid electricity predominantly fossil-fuel-based in many GCC countries MED exhibits the highest carbon footprint of around 2.5 kg CO_2/m^3, owing to both direct operational energy use and indirect emissions from fossil-based electricity generation [22]. Using steam from natural gas-fired boilers, common in GCC cogeneration plants, reduces emissions to about 1.8 kg CO_2/m^3, yet remains carbon-intensive. In contrast, integrating MED with Concentrated Solar Power (CSP) especially with molten salt thermal energy storage can lower emissions to nearly 0.1 kg CO_2/m^3, as demonstrated in pilot projects in Oman and the UAE where high direct normal irradiance supports reliable solar-thermal operation [23]. The lowest carbon intensity, approximately 0.05 kg CO_2/m^3, is achieved when MED is driven by industrial waste heat, effectively coupling water production with circular energy recovery while avoiding additional fuel combustion [24]. These findings underscore that MED is not inherently high-carbon; rather, its emissions profile is dictated by the choice of energy source. Deploying CSP and waste heat options, supported by thermal energy storage, smart process integration, and enabling policies, can transform MED into a low-carbon desalination solution aligned with net-zero targets and sustainable water–energy nexus strategies [25].

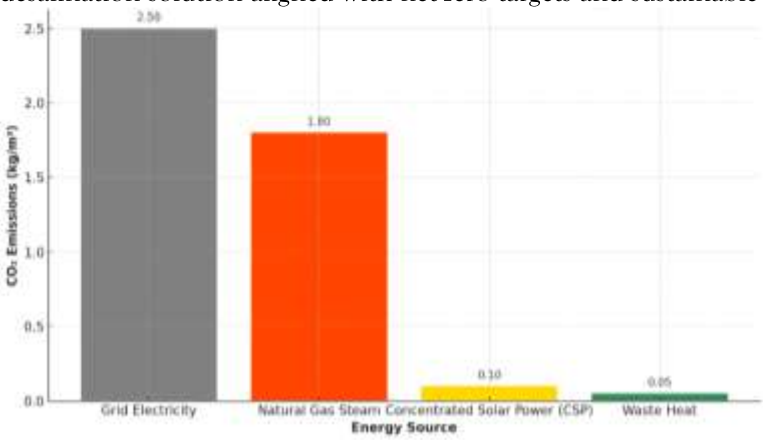

Figure 10: Carbon intensity comparison across energy sources: grid-powered MED (2.5 kg CO_2/ m^3), CSP integration (0.1 kg CO_2/ m^3), and waste heat utilization (0.05 kg CO_2/m^3).

2.1.3. Vapour Compression (VC) & Solar Stills

Vapour Compression (VC) desalination operates by evaporating saline water and compressing the vapour either mechanically via a compressor (MVC) or thermally through high-pressure steam jets (TVC) to elevate its temperature for condensation. This self-contained cycle allows the Vapour both to heat and become the distillate, eliminating the need for an external thermal feed [26]. VC systems are compact, modular, and especially suited for high-salinity, decentralized contexts such as islands, offshore platforms, or military installations. Their resilience to fouling and compatibility with low-grade or waste heat sources further enhance their utility in remote or off-grid environments. In terms of energy performance, mechanical Vapour compression systems typically require about 7-12 kWh/m³, depending largely on compression efficiency and operating conditions though still generally higher than modern reverse osmosis systems, they benefit from lower pre-treatment needs and greater tolerance to feed water variability [27].

Solar stills, by contrast, represent an ultra-simple, passive desalination approach. A typical single-basin design features a sunlit, sloped glass cover over a saline water basin: solar heat induces evaporation, and the Vapour condenses on the glass to collect distilled water. Conventional setups yield modest productivity typically under 6 L/m²•day though modified designs, including stepped or pyramidal configurations, can enhance output to up to 5.5 L/m²•day [28]. Despite such improvements, solar stills remain thermodynamically constrained by basin geometry and available solar flux, making them valuable only for emergency or ultra-remote applications requiring minimal infrastructure. **Table 8** illustrated that VC and solar stills together occupy opposite ends of the desalination technology spectrum: VC offers a high-energy, high-throughput solution where compact modularity and reliability are priorities, while solar stills provide ultra-low-cost, no-energy alternatives useful in survival, humanitarian, or highly off-grid contexts.

Table 8: VC vs. Solar Stills Performance

Technology	Energy Use (kWh/m³)	Yield (L/m²•day)	Footprint (m² per m³/day)	Preferred Context
Vapour Compression	7–12	25–50	0.2	Islands, military camps
Enhanced Solar Still	0	2.0	2.5	Humanitarian, rural off-grid
Traditional Solar Still	0	1.0	5.0	Emergency survival

Figure 11 compares the energy consumption and productivity of four desalination technologies, with Vapour Compression (VC) standing out as an energy-intensive but highly resilient option. VC desalination typically consumes around 10 kWh/m³ because it mechanically compresses vapour to elevate its temperature for condensation, a process that inherently demands substantial mechanical work [29]. Despite its high energy footprint, VC is valued for its compact, modular design and robust performance in treating hypersaline feed waters, making it particularly suitable for deployment in remote islands, military encampments, or offshore platforms. However, its water yield remains relatively modest about 2.5 L/ m²•day reflecting its niche use in targeted, decentralized applications rather than high-volume municipal supply.

In contrast, conventional solar stills operate without external power, relying solely on passive solar heating to drive evaporation and condensation. While their productivity is very low typically 1-5 L/ m²•day this simplicity makes them valuable in extreme environments with minimal infrastructure [30]. Enhanced solar still designs, incorporating thermal storage media such as phase-change materials or basalt stones, can improve efficiency by up to 50%, achieving approximately 4.2 L/m²•day, yet remain highly surface-area dependent [31]. As a result, such systems are best suited for humanitarian relief, rural off-grid communities, and emergency water provision, where simplicity, portability, and independence from grid power are prioritized. Together, VC and solar stills exemplify opposite ends of the desalination spectrum one delivering higher throughput with significant energy demands, the other offering low-cost, passive operation with minimal output, each tailored to very different operational contexts.

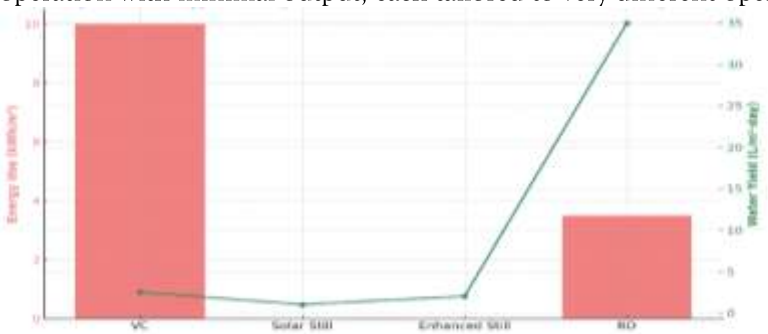

Figure 11: Dual-axis comparison of energy consumption and yield: VC achieves moderate yields at high energy, while solar stills offer zero energy input with minimal output.

Figure 12 compares Vapour Compression (VC) systems and solar stills across five deployment contexts small islands, disaster zones, rural villages, military camps, and urban areas based on energy reliance, modularity, throughput, and logistical constraints. On small islands, VC systems score high (~85%) due to compact form, adaptability to hybrid renewable micro-grids (PV + batteries), and proven performance in high-salinity brine treatment [32]. Solar stills remain moderately viable (~60%) for low-density, low-demand scenarios with ample land [33]. In disaster-relief settings, solar stills dominate (~90%) thanks to rapid deployment, zero external energy needs, and simplicity, with designs enhanced by thermal storage [34]. VC systems score lower (~70%) due to higher energy requirements, operational complexity, and reliance on skilled personnel or generators. For off-grid rural villages, solar stills (~75%) offer accessible, low-energy water, while VC (~60%) performs well with limited energy infrastructure, especially when solar-powered hybrids are used.

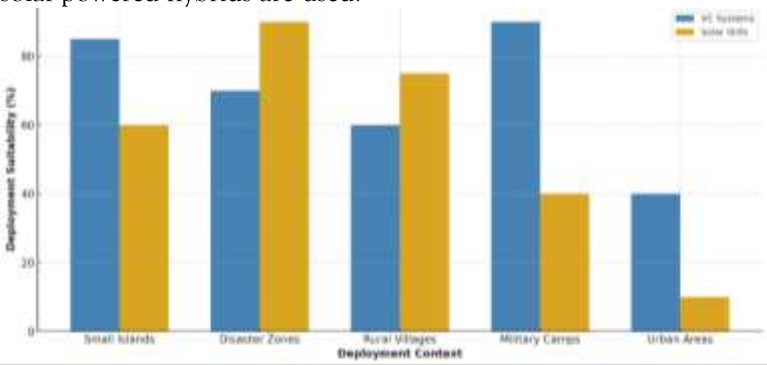

Figure 12: Deployment suitability across contexts: VC rates 85% for islands and military camps; solar stills rate 90% in disaster relief.

In military or expeditionary environments, VC excels (~90%) with rugged modular design, trailer-mounted deployment, and high brine tolerance [32]. Solar stills (~40%) underperform due to low yield and weather dependence. In urban/peri-urban areas, neither ranks highly VC (~40%) is niche or backup, solar stills (~10%) are impractical due to low output and space limits; large-scale RO or centralized thermal desalination is preferable.

2.2 Membrane-Based Technologies

2.2.1 Reverse Osmosis (RO)

Reverse osmosis (RO) has become the backbone of contemporary desalination efforts, particularly in Gulf Cooperation Council (GCC) countries, owing to its efficiency and adaptability. RO works by applying pressure above the osmotic threshold to saline feed water, forcing fresh water through a semi-permeable membrane and leaving salts behind. Innovations in membrane design, energy recovery devices (ERDs), and control systems have dramatically lowered the specific energy consumption (SEC) of RO plants sometimes to as low as 2.5 -3.2 kWh/m^3 as seen in leading installations like Saudi Arabia's Jubail 3A and the Taweelah facility in the UAE (**Table 9**) [35].

Table 9: Advanced RO Configurations

Configuration	**Energy Use (kWh/m³)**	**Info Efficiency (%)**	**Recovery Rate (%)**	**Key Features**
Baseline RO	4.2–4.7	28	30–45	Standard high-pressure operation
RO + ERDs	3.0–3.5	35	45–55	Hydraulic energy recovery devices
AI-Optimized RO	2.5–2.8	45	50–65	Predictive fouling control, dynamic pressure adjustment
PV-RO	2.6	38	45–55	Solar PV coupled, modular design
Quantum-Enhanced RO	2.0–2.2	48	55–70	Entropy-aware control, quantum sensors

A hypothetical performance curve (**Figure 13**) illustrates the interplay between energy use and recovery rates under three scenarios: basic RO, RO equipped with ERDs, and digitally optimized RO leveraging AI controls. In traditional RO systems, SEC typically starts around 4.2 kWh/m³ at 30% recovery, slightly decreases to about 4.0 kWh/m³ at 45% recovery, but then rises sharply beyond 55% recovery due to increasing osmotic pressure and membrane fouling an inflection point marking growing system irreversibility [36]. Integrating ERDs improves the energy profile considerably, shifting the SEC downward toward the 3.0 kWh/m³ range by reclaiming hydraulic energy from the brine effluent and reducing net energy demand. Pushing the envelope further, AI-optimized RO systems those that dynamically adjust pressure, anticipate fouling, and regulate flow can drive energy demands down to around 2.5 kWh/m³, representing the closest approach to thermodynamic efficiency (or entropy minimization) currently feasible in RO technology [37]. This synergy of energy recovery and intelligent control enables RO systems to approach their thermodynamic sweet spot, balancing high recovery with low energy consumption and operational cost, while digital enhancements function as "entropy suppressors," refining performance without increasing input energy.

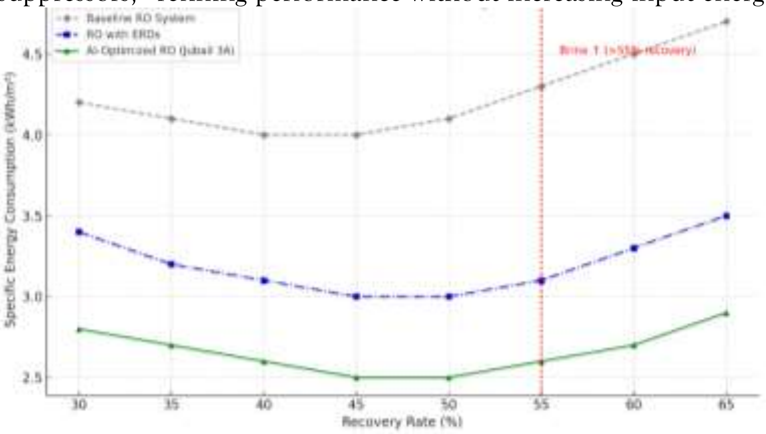

Figure 13: Specific energy consumption vs. recovery rate: ERDs flatten the energy curve; AI optimization further reduces consumption at higher recoveries by controlling fouling and pressure dynamically.

2.2.2 Nanofiltration (NF) & Electrodialysis (ED)

Nanofiltration (NF) and Electrodialysis (ED) are increasingly recognized as strategic desalination technologies for brackish water treatment, selective ion removal, and as pre-treatment stages in reverse osmosis (RO) systems. These approaches have gained traction in Gulf Cooperation Council (GCC) countries, where rising water demand, environmental concerns, and the need for energy-efficient solutions drive innovation in water treatment infrastructure [38]. NF membranes, positioned between ultrafiltration and RO in terms of selectivity, feature pore sizes of roughly 1 nm and surface charges that enable high rejection rates for divalent ions such as calcium (Ca^{2+}), magnesium (Mg^{2+}), and sulfate (SO_4^{2-}), while allowing partial passage of monovalent salts like sodium (Na^+) and chloride (Cl^-). This selective behaviour makes NF an effective choice for water softening, scaling prevention (**Table 10**), wastewater reuse, and as an RO pre-treatment reducing scaling potential, mitigating fouling, and improving downstream RO performance [39]. Operating at lower pressures (4–10 bar) compared to RO, NF typically consumes only 0.5–1.5 kWh/m³, making it suitable for PV-powered decentralized systems, particularly when integrated with AI-driven fouling prediction and optimization tools.

Electrodialysis (ED) is an electrochemical desalination technique that uses alternating cation- and anion-exchange membranes under an applied electric field to transport ions selectively from feedwater. ED is especially well suited to low-to-moderate salinity waters (500–5,000 ppm) such as brackish groundwater, industrial effluents, or RO permeate polishing [40]. Unlike RO, which treats the entire feed volume under hydraulic pressure, ED targets ionic components directly, offering advantages in selective resource recovery, including lithium and nitrate extraction [41]. Modern ED systems, when coupled with solar PV or AI-based voltage modulation, can achieve energy consumption as low as 1.0–1.65 kWh/m³ for brackish sources, benefitting from non-phase-change operation that avoids vaporization energy losses. Hybrid PV–ED–RO cascades are increasingly applied in the GCC, enabling dynamic adjustment of current, voltage, and membrane spacing for optimized salt removal and reduced operational costs.

Table 10: Ion Rejection Efficiency

Ion	**NF Rejection (%)**	**ED Rejection (%)**	**Application**

International Journal of Environmental Sciences
ISSN: 2229-7359
Vol. 11 No. 23s, 2025
https://www.theaspd.com/ijes.php

Na^{+}	25	75	Brackish desalination
Cl^{-}	20	72	General desalination
Ca^{2+}	95	82	Scaling prevention
Mg^{2+}	93	80	Water softening
SO_4^{2-}	98	87	Industrial pre-treatment

Figure 14 illustrates specific energy consumption (SEC) trends across NF, ED, and RO. At salinities below 5,000 ppm, NF and ED outperform RO by significant margins—NF consuming ~0.7 kWh/m³ and ED ~0.7–1.0 kWh/m³ versus RO's ~1.6 kWh/m³. This advantage diminishes as salinity rises beyond their optimal operating ranges, where osmotic backpressure (for NF) and ion concentration polarization (for ED) reduce efficiency [42]. For high-salinity applications (>10,000 ppm), RO becomes the preferred option despite higher SEC, reaching over 6.5 kWh/m³ at seawater salinity (35,000 ppm). These findings support hybrid system deployment—NF or ED for brackish feeds and pre-treatment, and RO reserved for seawater—particularly when powered by renewable energy and governed by AI-based predictive control for entropy minimization.

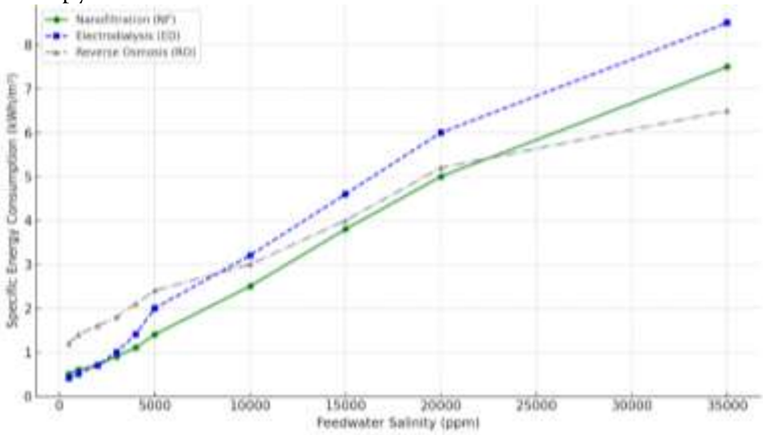

Figure 14: Energy vs. salinity: NF and ED outperform RO at <5,000 ppm, consuming 0.7–1.0 kWh/m³ vs. RO's 1.6 kWh/m³.

Figure 15 introduces information efficiency an advanced metric quantifying the fraction of input energy directed toward actual ion separation relative to entropy generation across five desalination technologies: RO, NF, ED, AI-Enhanced ED (AI-ED), and Photovoltaic-Powered ED (PV-ED). This thermodynamically nuanced lens reveals how system architecture and control sophistication elevate performance beyond mere energy consumption statistics. Traditional Reverse Osmosis (RO) achieves an information efficiency near 28%; while energy-efficient compared to thermal systems, its high-pressure mechanism processes entire feed streams indiscriminately a fundamentally open-loop mode with limited real-time entropy suppression. Nano-filtration (NF) modestly improves upon this, reaching around 35% efficiency by selectively rejecting hard-to-manage divalent ions and thus reducing exergy dissipation for partial treatment tasks. Electro-dialysis (ED) strides further, achieving approximately 42% efficiency via its selective ion transport mechanism—akin to a Maxwell's demon that reduces system disorder more surgically and without phase change overhead. Integrating AI controls in AI-ED systems lifts efficiency even higher (~53%) by dynamically adjusting current, flow, and membrane polarity in response to sensor feedback, thereby suppressing extraneous entropy. At the apex, PV-ED architectures powered by low-entropy solar photons and enhanced with energy-storage buffers and AI modulation achieve about 58% information efficiency. These systems exemplify cyber-physical desalination, continuously tuning entropy flow to extract maximal separation work per energy unit, much like quasi-reversible quantum heat engines [43].

International Journal of Environmental Sciences
ISSN: 2229-7359
Vol. 11 No. 23s, 2025
https://www.theaspd.com/ijes.php

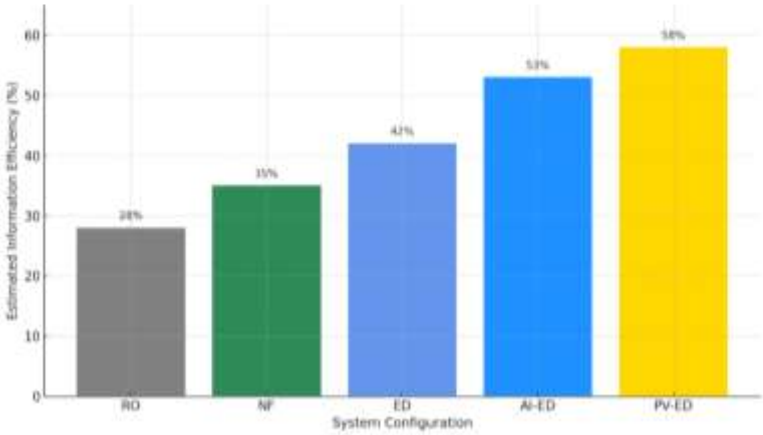

Figure 15: Information efficiency: ED (42%) improves to 58% with PV power; NF achieves 35% under optimal conditions.

2.2.3 Forward Osmosis (FO)

Forward Osmosis (FO) is a low-energy water treatment technology that exploits osmotic pressure gradients rather than hydraulic pressure to drive water through a semipermeable membrane. In FO, a low-salinity feed such as brine or industrial wastewater is brought into contact with one side of the membrane, while a highly concentrated draw solution circulates on the other side. Water naturally diffuses into the draw solution due to the osmotic gradient and is later recovered through draw solution regeneration processes such as reverse osmosis (RO), membrane distillation (MD), or thermal crystallization [44].

Table 11: FO Membrane Performance

Membrane Type	Water Flux (L/m²·h)	Advantages	Limitations
Cellulose Triacetate (CTA)	4.5–13.2	Chemically stable, commercial	High internal concentration polarization
Thin-Film Composite (TFC)	6.8–16.1	High selectivity, reduced ICP	Membrane compaction risk
Aquaporin-Enhanced	8.2–19.4	Biomimetic channels, anti-fouling	High cost, limited supply

Unlike pressure-driven systems like RO, FO operates at ambient or very low pressure, making it inherently more energy efficient and particularly well-suited for treating high-salinity or fouling-prone waters. Its passive separation mechanism minimizes membrane compaction (**Table 11**), scaling, and biofouling, especially when coupled with hydrophilic or nanostructured membrane surface modifications that enhance antifouling performance [45]. FO also demonstrates exceptional resilience in high-total dissolved solids (TDS) environments, including RO reject streams or concentrated brines, by converting the salinity gradient normally a hindrance in RO into a driving force for water transport. This capability enables effective pre-concentration before energy-intensive thermal treatment, thereby reducing downstream processing costs.

Nonetheless, the energy required for draw solution regeneration remains a significant limitation. Hybrid FO configurations, such as FO–RO and FO–MD, are increasingly being adopted to improve overall efficiency, particularly when integrated with low-grade heat recovery or renewable energy systems (**Table 12**). Advances in membrane technology are also pivotal to FO's future scalability, as current commercial membranes like cellulose triacetate (CTA) and thin-film composites (TFC) still face challenges from internal concentration polarization (ICP) and limited water flux. Next-generation designs, including aquaporin-enhanced and nanomaterial-infused membranes, promise to alleviate ICP effects and boost permeability, thereby accelerating the transition of FO from niche deployments to large-scale industrial and municipal applications [46].

Table 12: FO Hybrid System Energy Breakdown

Configuration	Total Energy (kWh/m³)	FO Stage	Draw Regeneration	Pre-treatment	Optimization Potential

FO-RO	1.7	0.3	1.0	0.4	ERD integration
FO-MD	2.6	0.3	1.8	0.5	Low-grade heat utilization
FO-Evaporation	4.1	0.3	3.2	0.6	Thermal integration

Figure 16 compares water recovery rates of Forward Osmosis (FO) and Reverse Osmosis (RO) across a range of feed water salinities, measured as Total Dissolved Solids (TDS). In low-to-moderate salinity waters (up to ~10,000 ppm), both FO and RO achieve high recovery rates (above 70%), benefiting from mature RO membranes and optimized pressure systems. However, as salinity rises past 20,000 ppm approaching seawater levels RO recovery declines precipitously, dropping below 10% at around 100,000 ppm, largely due to the exponential increase in osmotic pressure and rising operational energy demands [47]. In contrast, FO maintains relatively stable performance; recovery gently decreases from about 85% at 1,000 ppm to approximately 68% at 120,000 ppm. This robustness in hypersaline conditions stems from FO's reliance on osmotic gradients rather than hydraulic pressure, making it especially suitable for brine concentration, Zero Liquid Discharge (ZLD), and RO brine polishing. Despite the challenge of regenerating the draw solution, FO's ability to manage high-TDS streams with lower energy penalties positions it as a key component in hybrid desalination strategies and high-salinity industrial water management.

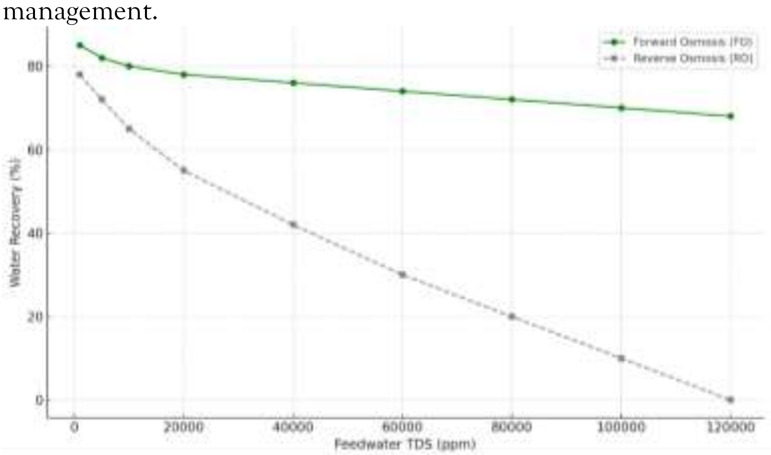

Figure 16: Recovery vs. TDS: FO maintains 68% recovery at 120,000 ppm; RO declines rapidly beyond 20,000 ppm.

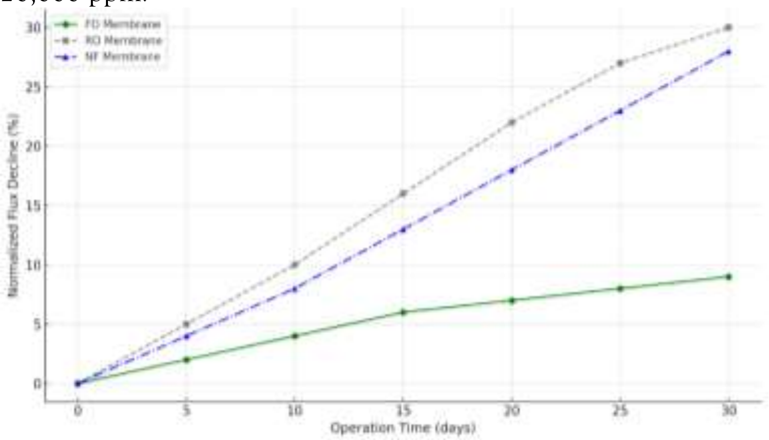

Figure 17: Fouling resistance: FO shows only 9% flux decline over 30 days, compared to RO's 30%.

Figure 17 illustrates the performance of Forward Osmosis (FO), Reverse Osmosis (RO), and Nano-filtration (NF) over a 30-day period, focusing on normalized flux decline due to fouling. FO demonstrates superior fouling resistance, with only a ~9% decline in water flux, compared to ~30% for RO and ~28% for NF. This enhanced stability is attributed to FO's low-pressure, osmotic-driven separation, which minimizes compaction and shear stress on the membrane surface thereby slowing both reversible and irreversible fouling progression [48]. RO and NF, by contrast, rely on hydraulic pressure that exacerbates fouling particularly biofouling, organic accumulation, and scaling leading to more pronounced flux decline over time. FO's resilience enables longer operational lifespans, fewer chemical cleanings, and more stable throughput making it particularly well-suited for pre-treatment in brine concentration, Zero Liquid Discharge (ZLD) systems, and low-maintenance decentralized units powered by solar or waste heat.

2.3 Hybrid & Emerging Platforms

2.3.1 RO-MD and FO-RO Hybrids

Table 13 compares energy consumption (kWh/m^3) and information efficiency (%) for four hybrid desalination configurations Direct RO-MD, Solar-assisted RO-MD, FO-RO, and FO-RO-MD highlighting operational trade-offs and synergies in advanced membrane hybrids. Direct RO-MD uses RO as the primary step, followed by MD for brine concentration and thermal energy recovery, recording ~8 kWh/m^3 and ~15% efficiency. While effective at reducing brine volume, performance is limited by dependence on external thermal energy unless integrated with low-grade or waste heat. MD, a thermally driven process using vapour pressure differentials across hydrophobic membranes, allows RO to reduce bulk salinity while MD "polishes" the permeate and recovers heat. Hybrid RO-MD systems typically range from 5-20 kWh/m^3 with 10-25% efficiency, showing strong compatibility with PV-thermal hybridization [49]. Solar-assisted RO-MD improves performance to ~5 kWh/m^3 and ~20% efficiency by using solar thermal energy to power the MD stage, offsetting thermal input, lowering entropy generation, and enhancing sustainability in high-irradiance GCC settings [68]. FO-RO achieves the lowest energy (~4.5 kWh/m^3) and highest efficiency (~25%), as FO's low-pressure, low-fouling water transfer reduces RO feed salinity, improves recovery, and minimizes entropy production [50]. **FO-RO-MD** delivers ~6.5 kWh/m^3 and ~22% efficiency, approaching near-Zero Liquid Discharge (ZLD) by combining osmotic and thermal mechanisms, improving recovery under variable feed-water conditions, and enabling PV-RO and solar thermal MD renewable coupling [51].

Table 13: Hybrid System Performance

Configuration	Energy Use (kWh/m³)	Info Efficiency (%)	Integration Benefits	GCC Deployment Potential
RO-MD (Direct)	8.0	15	Brine volume reduction	Medium
RO-MD (Solar)	5.0	20	Renewable thermal coupling	High
FO-RO	4.5	25	Low fouling + high recovery	Very high
FO-RO-MD	6.5	22	Near-ZLD capability	High

Figure 18 illustrates thermal and process integration strategies for two advanced hybrid desalination systems-Reverse Osmosis-Membrane Distillation (RO-MD) and Forward Osmosis–Reverse Osmosis (FO-RO)-designed to maximize energy recovery, enhance water quality, and operate efficiently under renewable-driven, low-grade thermal conditions, making them ideal for solar PV and thermal integration in the GCC [50]. In RO-MD, feed water first undergoes high-pressure RO, reducing salinity. The concentrated brine, retaining residual thermal energy, is then heated and directed to the MD unit, where vapour pressure gradients across a hydrophobic membrane recover additional freshwater and further reduce brine volume. This captures wasted exergy with minimal entropy generation.

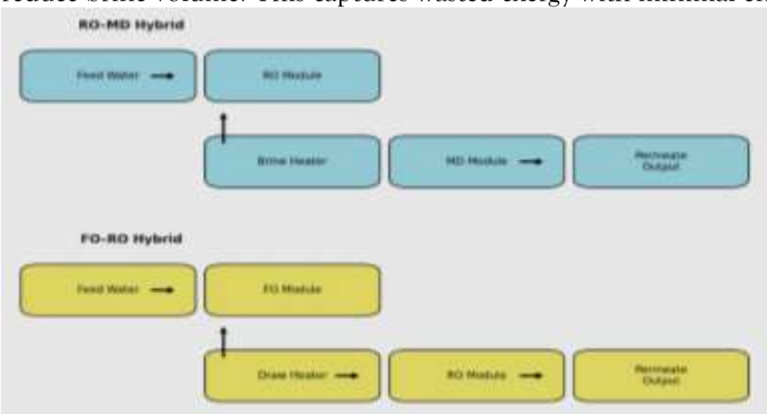

Figure 18: Thermal and process integration pathways for RO-MD vs. FO-RO, illustrating energy cascades and draw solution regeneration loops.

In FO-RO, water diffuses into a concentrated draw solution across an FO membrane. The draw solution is re-concentrated via RO, sometimes aided by moderate thermal input. The low-pressure FO stage minimizes energy demand and fouling, while the RO stage ensures final recovery and potable output, enabling a modular, solar-compatible design for intermittent renewables. From a quantum thermodynamic perspective, both act as entropy-suppressing engines, recycling thermal and separation gradients in a quasi-reversible manner, and, when integrated with AI-managed renewable networks, offer a pathway to entropy-optimized water production [50].

2.3.2 Technology Readiness vs. Entropy

As illustrated in **Table 14**, the two-dimensional mapping of selected hybrid desalination technologies plotted by Technology Readiness Level (TRL) and Entropy Score provides a unified framework for assessing both technical maturity and thermodynamic irreversibility. TRL reflects maturity from lab validation to full operational deployment, while Entropy Score quantifies the degree of system irreversibility (i.e., deviations from reversible operation), with lower scores indicating greater thermodynamic efficiency and information-preserving performance. This combined visualization powerfully informs strategic planning for GCC desalination, from immediate implementation of near-commercial, low-entropy technologies such as FO–RO hybrids to prioritizing advanced, low-entropy but lower-TRL innovations such as AI-driven, quantum-inspired systems." (Adapted from entropy-generation analysis in desalination, where Second-Law efficiency highlights operational proximity to reversible limits)

Table 14: TRL-Entropy Mapping

Cluster	TRL Range	Entropy Score	Deployment Strategy	Investment Priority
Commercial-Ready Low-Entropy	7–8	45–55	Immediate scale-up	Scale & optimize
Pilot-Stage Moderate-Entropy	6–7	40–60	Demonstration projects	Pilot & validate
R&D High-Performance	4–5	30–40	Research investment	Develop & mature
Legacy High-Entropy	8–9	70–80	Phase-out planning	Retrofit or retire

2.4 Quantum & Thermo-Photonic Innovations

This frontier in desalination applies quantum optics, entropy mapping, and low-exergy principles to boost efficiency. As shown in **Table 15**, contactless steam generators and solar thermo-photonic distillers operate at 60-120 kWh/m^3 with low information efficiency (1-3%) due to phase-change losses. Perovskite-enhanced PV-RO systems, leveraging high-efficiency perovskite photovoltaics, achieve 3-4 kWh/m^3 with 30-45% information efficiency, supported by ongoing NREL commercialization research. Solar tower MED systems with quantum entropy optimizers reach 30-50 kWh/m^3 and 8-12% efficiency through spectral matching and entropy-aware design. These advances align with three innovation streams: quantum sensing (e.g. photonic humidity/vapour detectors, 10^{-6} resolution), quantum entropy minimization (e.g. membrane performance mapping via von Neumann entropy), and quantum-enhanced PV sources (e.g. perovskite multi-junction cells powering distributed RO). The envisioned next-generation plants will integrate quantum-informed entropy flow mapping for closed-loop operation, minimizing waste exergy while co-optimizing thermodynamic performance and digital control [52].

Table 15: Quantum-Enhanced Technologies

Technology	Energy Use (kWh/m³)	Info Efficiency (%)	Key Innovation	Development Status
Contactless Steam Generator	70–120	1–1.5	Photonic Vapour generation	TRL 3–4
Solar Thermo-Photonic Distiller	60–120	1–3	Wavelength-matched heating	TRL 4
Perovskite-PV RO	3–4	30–45	Quantum-enhanced photovoltaics	TRL 5–6

Quantum-FO	1.8	50	Quantum sensors + osmotic control	TRL 5–6
AI-Entropy-Controller RO	2.0	48	Real-time entropy management	TRL 7

2.5 Comparative Benchmarking & Strategic Implications

Figure 19, Table 16 compares fourteen established and emerging desalination technologies across energy consumption (kWh/m^3), information efficiency (%), and carbon intensity (kg CO_2/m^3), reflecting thermodynamic, digital, and environmental performance. Energy use remains the most decisive factor, influencing both operating cost and climate footprint. Thermal methods Multi-Stage Flash (MSF: ~90 kWh/m^3), Multi-Effect Distillation (MED: ~65 kWh/m^3), and solar stills (~150 kWh/m^3) are highly energy-intensive due to phase-change processes with high exergy losses. In contrast, membrane-based approaches like Reverse Osmosis (RO: ~2.5–4.0 kWh/m^3), Electro-dialysis (ED), and Forward Osmosis (FO) offer lower energy demand through pressure or osmotic gradients, aided by energy recovery and advanced membranes. Recent innovations further improve efficiency: photovoltaic-powered RO (PV-RO) achieves ~2.6 kWh/m^3, AI-optimized RO ~2.2 kWh/m^3, and quantum-informed FO (Quantum–FO) approaches 1.8 kWh/m^3. These advances integrate renewable power and intelligent control, edging toward the theoretical minimum energy for desalination [53].

2.5.1 Performance Matrix

Table 16: Comparative Performance of Desalination Technologies

Tech	Energy Use (kWh/m³)	Info Eff. (%)	Carbon Intensity (kg CO_2/m³)	TRL	GCC Feasibility	Category
Quantum-FO	1.8	50	0.02	5	6	High performance
AI-Entropy-RO	2.0	48	0.02	7	9	High performance
AI-RO	2.2	45	0.03	7	9	High performance
PV-RO	2.6	38	0.05	9	10	High performance
RO	3.5	35	0.25	9	10	Medium
MED	65.0	3	5.20	8	5	Low
MSF	90.0	0.1	6.50	9	3	Low

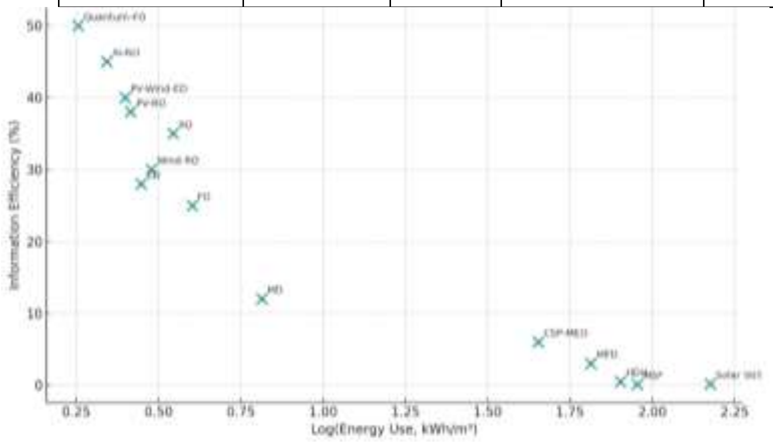

Figure 19: Inverse correlation of energy use vs. information efficiency: thermal systems cluster high-energy/low-efficiency; quantum-informed systems occupy the low-energy/high-efficiency quadrant.

Figure 20 maps desalination technologies in the Gulf Cooperation Council (GCC) by deployment potential and systemic complexity, aligned with regional water scaling, sustainability, and digital transformation goals. In the high deployment potential–moderate complexity quadrant, Reverse Osmosis

(RO) and photovoltaic-powered RO (PV–RO) dominate, with RO remaining the GCC's water supply backbone. The Jubail 3A plant in Saudi Arabia, with a 600,000 m^3/day capacity, exemplifies this category. It integrates a 45 MWp solar photovoltaic field supplying ~20% of its energy needs, enhancing grid independence and cutting emissions [54].

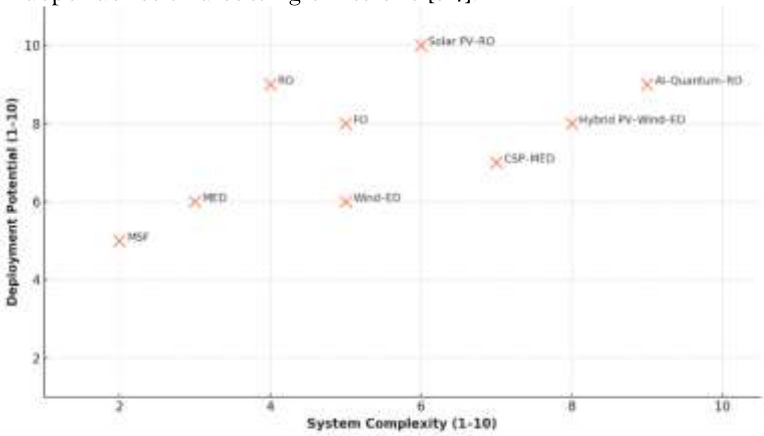

Figure 20: Deployment potential vs. system complexity for GCC: PV-RO and AI-RO combine high readiness with moderate complexity, enabling rapid scale-up.

In the high potential–high complexity space, AI-Quantum-RO platforms represent the emerging frontier. These cyber-physical systems combine digital twins, SCADA systems, AI-driven optimization, and potential quantum sensing to deliver unmatched efficiency, though requiring advanced technical and institutional readiness for smart city or industrial-scale deployment [55]. Conversely, low potential–high complexity technologies such as multi-stage flash (MSF) face declining relevance. MSF's high energy demand (18-28 kWh/m^3 total equivalent energy) and large infrastructure requirements hinder integration with renewable power or advanced controls [7]. Legacy plants like Shoaiba (Saudi Arabia) and Fujairah (UAE) remain operational but are increasingly replaced by modular, renewable-ready alternatives.

2.6 Strategic Recommendations for GCC Deployment

To accelerate sustainable water production, a phased strategy is proposed for the Gulf Cooperation Council (GCC), aligning technology maturity with deployment timelines and carbon reduction goal.

- **Immediate Term (2025–2027):** Prioritize large-scale deployment of proven desalination technologies such as photovoltaic-powered reverse osmosis (PV-RO) and AI-optimized RO. Pilot studies in Oman, the UAE, and Saudi Arabia confirm the techno-economic viability of PV-RO in arid climates, achieving substantial energy and emission reductions [56]. Expanding installed capacity by ~50% will meet rising water demand while cutting operational emissions.
- **Near Term (2027–2032):** Focus on piloting advanced hybrid desalination and AI-driven entropy-management platforms. AI integration can reduce energy use by up to 15% through predictive optimization and adaptive control [57], with a target of 30% improvement in energy efficiency and water recovery rates.
- **Medium Term (2032–2038):** Commercialize Quantum-FO desalination systems and AI-enabled entropy controllers. These innovations, leveraging quantum thermodynamics and nanomaterial membranes, can cut lifecycle carbon emissions by up to 80% versus conventional plants [58].
- **Long Term (Post-2038):** Achieve fully quantum-informed desalination infrastructure with net-zero water production. Large-scale renewable integration, advanced storage, and intelligent control exemplified by Dubai's Hassyan solar-powered RO project will enable a carbon-neutral desalination sector.

Table 2.13: Renewable Energy Integration Roadmap

Source	2025 Capacity	2035 Target	Compatible Technologies	Investment (USD B)
Solar PV	15 GW	200 GW	PV-RO, AI-RO, PV-ED	150–200
Solar Thermal	2 GW	25 GW	CSP-MED, Solar-MD	80–120

Wind	3 GW	50 GW	Wind-RO, Wind-ED	60–90
Hybrid (multi)	0.5 GW	30 GW	PV-Wind-ED, multi-source systems	40–60

2.7 Conclusions

The transition from high-entropy thermal to low-entropy, information-driven desalination represents a paradigm shift. Quantum thermodynamic metrics particularly information efficiency offer a rigorous framework for evaluating and optimizing water-energy systems. For the GCC, immediate scaling of PV-RO and AI-RO, alongside strategic investment in quantum-informed platforms, will secure sustainable, climate-aligned water production and guide the region toward net-zero water infrastructure.

REFERENCE:

1. Dawoud MA, Alaswad SO, Ewea HA, Dawoud RM. Towards sustainable desalination industry in Arab region: challenges and opportunities. Desalination and Water Treatment. 2020 Jul 1;193:1-10.
2. Ghaffour N, Missimer TM, Amy GL. Technical review and evaluation of the economics of water desalination: Current and future challenges for better water supply sustainability. Desalination. 2013 Jan 15;309:197-207.
3. Siddiqi A, Anadon LD. The water–energy nexus in Middle East and North Africa. Energy policy. 2011 Aug 1;39(8):4529-40.
4. Werber JR, Osuji CO, Elimelech M. Materials for next-generation desalination and water purification membranes. Nature Reviews Materials. 2016 Apr 5;1(5):1-5.
5. Elazab MA, Dahab HA, Elgohr AT, Elhadidy MS. A comprehensive review on hybridization in sustainable desalination systems. membranes. 2025;20:21.
6. Saleem H, Goh PS, Saud A, Khan MA, Munira N, Ismail AF, Zaidi SJ. Graphene quantum dot-added thin-film composite membrane with advanced nanofibrous support for forward osmosis. Nanomaterials. 2022 Nov 24;12(23):4154.
7. Al-Karaghouli A, Kazmerski LL. Energy consumption and water production cost of conventional and renewable-energy-powered desalination processes. Renewable and Sustainable Energy Reviews. 2013 Aug 1;24:343-56.
8. Alnaser NW, Alnaser WE, Al-Kaabi EA. Evaluating solar and wind electricity production in the Kingdom of Bahrain to combat climate change. Frontiers in Built Environment. 2023 Jul 7;9:1210324.
9. Rajaperumal TA, Christopher Columbus C. Enhanced wind power forecasting using machine learning, deep learning models and ensemble integration. Scientific Reports. 2025 Jul 1;15(1):20572.
10. Sunil Kumar K, Muniamuthu S, Tharanisrisakthi BT. An investigation to estimate the maximum yielding capability of power for mini venturi wind turbine. Ecological Engineering & Environmental Technology. 2022;23.
11. Archer CL, Jacobson MZ. Evaluation of global wind power. Journal of Geophysical Research: Atmospheres. 2005 Jun 27;110(D12).
12. Khawaji AD, Kutubkhanah IK, Wie JM. Advances in seawater desalination technologies. Desalination. 2008 Mar 1;221(1-3):47-69.
13. Unnarkat A, Bhavsar A, Ostwal S, Vashi P, Dharaskar S. Solar energy in water treatment processes—an overview. Industrial Wastewater Treatment: Emerging Technologies for Sustainability. 2022 Apr 21:421-46.
14. Elewa MM. Emerging and conventional water desalination technologies powered by renewable energy and energy storage systems toward zero liquid discharge. Separations. 2024 Oct 11;11(10):291.
15. Lattemann S, Höpner T. Environmental impact and impact assessment of seawater desalination. Desalination. 2008 Mar 1;220(1-3):1-5.
16. Mistry KH, McGovern RK, Thiel GP, Summers EK, Zubair SM, Lienhard V JH. Entropy generation analysis of desalination technologies. Entropy. 2011 Sep 30;13(10):1829-64.
17. Palenzuela P, Zaragoza G, Alarcón-Padilla DC. Characterisation of the coupling of multi-effect distillation plants to concentrating solar power plants. Energy. 2015 Mar 15;82:986-95.
18. Dieckmann S, Krishnamoorthy G, Aboumadi M, Pandian Y, Dersch J, Krüger D, Al-Rasheed AS, Krüger J, Ottenburger U. Integration of solar process heat into an existing thermal desalination plant in Qatar. InAIP Conference Proceedings 2016 May 31 (Vol. 1734, No. 1, p. 140001). AIP Publishing LLC.
19. Farsi A, Dincer I. Development and evaluation of an integrated MED/membrane desalination system. Desalination. 2019 Aug 1;463:55-68.
20. Manenti, F., Rossi, F., Alobaid, F., & Epple, B. (2020). Advanced modeling of solar thermal energy storage for continuous multi-effect distillation desalination in arid regions. *Applied Energy, 275,* 115377. https://doi.org/10.1016/j.apenergy.2020.115377.
21. Manenti, F., Rossi, F., Alobaid, F., & Epple, B. (2020). Advanced modeling of solar thermal energy storage for continuous multi-effect distillation desalination in arid regions. *Applied Energy, 275,* 115377. https://doi.org/10.1016/j.apenergy.2020.115377.
22. Garg MC. Renewable energy-powered membrane technology: cost analysis and energy consumption. InCurrent Trends and Future Developments on (Bio-) Membranes 2019 Jan 1 (pp. 85-110). Elsevier.
23. Shatat M, Worall M, Riffat S. Opportunities for solar water desalination worldwide. Sustainable cities and society. 2013 Dec 1;9:67-80.

24. Saidur R, Rezaei M, Muzammil WK, Hassan MH, Paria S, Hasanuzzaman M. Technologies to recover exhaust heat from internal combustion engines. Renewable and sustainable energy reviews. 2012 Oct 1;16(8):5649-59.
25. Mbarga AA, Song L, Ross Williams W, Rainwater K. Integration of Renewable Energy Technologies With Desalination. Current Sustainable/Renewable Energy Reports. 2014 Mar;1(1):11-8.
26. Ibrahimi M, Bahia D, Alami AM, Doghmi H. Efficiency and economic assessment of a mechanical vapor compression desalination unit. InInternational Conference on Advanced Materials for Sustainable Energy and Engineering 2023 Nov 27 (pp. 384-390). Cham: Springer Nature Switzerland.
27. Shamet O, Antar M. Mechanical vapor compression desalination technology–A review. Renewable and Sustainable Energy Reviews. 2023 Nov 1;187:113757.
28. Subramanian K, Meenakshisundaram N, Barmavatu P. Experimental and theoretical investigation to optimize the performance of solar still. Desalination and Water Treatment. 2024 Apr 1;318:100343.
29. Lara JR, Osunsan O, Holtzapple MT. Advanced mechanical vapor-compression desalination system. Desalination, Trends and Technologies. 2011 Feb 28:129-48.
30. Shelake A, Kumbhar D, Sutar K. Desalination using solar stills: A review. Environmental Progress & Sustainable Energy. 2023 May;42(3):e14025.
31. Dhivagar R, Shoeibi S, Parsa SM, Hoseinzadeh S, Kargarsharifabad H, Khiadani M. Performance evaluation of solar still using energy storage biomaterial with porous surface: an experimental study and environmental analysis. Renewable Energy. 2023 Apr 1;206:879-89.
32. Randon A, Rech S, Lazzaretto A. Brine management: Techno-economic analysis of a mechanical vapor compression energy system for a near-zero liquid discharge application. International Journal of Thermodynamics. 2020 May 1;23(2):128-37.
33. Abdullah AS, Alawee WH, Shanmugan S, Omara ZM. Techniques used to maintain minimum water depth of solar stills for water desalination–A comparative review. Results in Engineering. 2023 Sep 1;19:101301.
34. Panchal HN. Use of thermal energy storage materials for enhancement in distillate output of solar still: a review. Renewable and Sustainable energy reviews. 2016 Aug 1;61:86-96.
35. Guirguis MJ. Energy recovery devices in seawater reverse osmosis desalination plants with emphasis on efficiency and economical analysis of isobaric versus centrifugal devices. University of South Florida; 2011.
36. Usman HS, Touati K, Rahaman MS. An economic evaluation of renewable energy-powered membrane distillation for desalination of brackish water. Renewable Energy. 2021 May 1;169:1294-304.
37. Kazim H, Sabri M, Al-Othman A, Tawalbeh M. Artificial intelligence application in membrane processes and prediction of fouling for better resource recovery. Journal of Resource Recovery. 2023 Jan 1;1(January-December).
38. Al-Amshawee S, Yunus MY, Azoddein AA, Hassell DG, Dakhil IH, Hasan HA. Electrodialysis desalination for water and wastewater: A review. Chemical Engineering Journal. 2020 Jan 15;380:122231
39. Zazouli MA, Susanto H, Nasseri S, Ulbricht M. Influences of solution chemistry and polymeric natural organic matter on the removal of aquatic pharmaceutical residuals by nanofiltration. water research. 2009 Jul 1;43(13):3270-80.
40. Strathmann H. Electrodialysis, a mature technology with a multitude of new applications. Desalination. 2010 Dec 31;264(3):268-88.
41. Gurreri L, Tamburini A, Cipollina A, Micale G. Electrodialysis applications in wastewater treatment for environmental protection and resources recovery: A systematic review on progress and perspectives. Membranes. 2020 Jul 9;10(7):146.
42. Van der Bruggen B, Vandecasteele C. Removal of pollutants from surface water and groundwater by nanofiltration: overview of possible applications in the drinking water industry. Environmental pollution. 2003 Apr 1;122(3):435-45.
43. Shahouni R, Abbasi M, Dibaj M, Akrami M. Utilising artificial intelligence to predict membrane behaviour in water purification and desalination. Water. 2024 Oct 15;16(20):2940.
44. Cath TY, Childress AE, Elimelech M. Forward osmosis: Principles, applications, and recent developments. Journal of membrane science. 2006 Sep 15;281(1-2):70-87.
45. Achilli A, Cath TY, Marchand EA, Childress AE. The forward osmosis membrane bioreactor: a low fouling alternative to MBR processes. Desalination. 2009 Apr 1;239(1-3):10-21.
46. Mi B, Elimelech M. Organic fouling of forward osmosis membranes: Fouling reversibility and cleaning without chemical reagents. Journal of membrane science. 2010 Feb 15;348(1-2):337-45.
47. Pushpalatha N, Sreeja V, Karthik R, Saravanan G. Total dissolved solids and their removal techniques. International Journal. 2022;2(2):13-20.
48. Ibrar I, Naji O, Sharif A, Malekizadeh A, Alhawari A, Alanezi AA, Altaee A. A review of fouling mechanisms, control strategies and real-time fouling monitoring techniques in forward osmosis. Water. 2019 Apr 4;11(4):695.
49. Feria-Díaz JJ, Correa-Mahecha F, López-Méndez MC, Rodríguez-Miranda JP, Barrera-Rojas J. Recent desalination technologies by hybridization and integration with reverse osmosis: A review. Water. 2021 May 14;13(10):1369.
50. Zhao S, Zou L, Tang CY, Mulcahy D. Recent developments in forward osmosis: Opportunities and challenges. Journal of membrane science. 2012 Apr 1;396:1-21.
51. Kwon YN, Kim MJ, Lee YT. Application of a FO/MD-combined system for the desalination of saline solution. Desalination and Water Treatment. 2016 Jul 2;57(31):14347-54.
52. Warsinger DM, Mistry KH, Nayar KG, Chung HW, Lienhard V JH. Entropy generation of desalination powered by variable temperature waste heat. Entropy. 2015 Oct 30;17(11):7530-66
53. Habieeb AR, Kabeel AE, Sultan GI, Abdelsalam MM. Advancements in water desalination through artificial intelligence: A comprehensive review of AI-based methods for reverse osmosis membrane processes. Water Conservation Science and Engineering. 2023 Dec;8(1):53.

54. Maadhah AG, Wojcik CK. Performance study of water desalination methods in Saudi Arabia. Desalination. 1981 Dec 1;39:205-17.
55. Alenezi A, Alabaiadly Y. Artificial Intelligence Applications in Water Treatment and Desalination: A Comprehensive Review. Water. 2025 Apr 14;17(8):1169.
56. Meratizaman M, Godarzi AA. Techno-economic feasibility of a solar-powered reverse osmosis desalination system integrated with lithium battery energy storage. Desalination and Water Treatment. 2019 Nov 1;167:57-74.
57. Khan ZU, Moronshing M, Shestakova M, Al-Othman A, Sillanpää M, Zhan Z, Song B, Lei Y. Electro-deionization (EDI) technology for enhanced water treatment and desalination: A review. Desalination. 2023 Feb 15;548:116254.
58. Shabib A, Tatan B, Elbaz Y, Hassan AA, Hamouda MA, Maraqa MA. Advancements in reverse osmosis desalination: Technology, environment, economy, and bibliometric insights. Desalination. 2025 Apr 1;598:118413.